UNIVERSITY OF CALIFORNIA SAN DIEGO

Battery Operating Regimes: Effect of Temporal Resolution on Peak Shaving by Battery Energy Storage System

A thesis submitted in partial satisfaction of the
requirements for the degree
Master of Science

in

Engineering Sciences (Mechanical Engineering)

by

Shiyi Liu

Committee in charge:

Professor Jan Kleissl, Chair
Professor Michael Davidson
Professor Patricia Hidalgo-Gonzalez

2021

The thesis of Shiyi Liu is approved, and it is acceptable in quality and form for publication on microfilm and electronically.

University of California San Diego

2021

DEDICATION

Thanks to my family.

TABLE OF CONTENTS

LIST OF FIGURES

ACKNOWLEDGEMENTS

I would like to acknowledge Professor Jan Kleissl for his support as the chair of my committee. Through multiple drafts and discussions, his invaluable guidance leads me to the right path.

I would like to acknowledge Doctor Sushil Silwal from CER, UCSD, without whom the journey of this research would be more tough.

The thesis is currently being prepared for submission for publication of the material. Liu, Shiyi; Silwal, Sushil; Kleissl, Jan. The thesis author was the primary investigator and author of this material.

ABSTRACT OF THE THESIS

Battery Operating Regimes: Effect of Temporal Resolution on Peak Shaving by Battery Energy Storage System

by

Shiyi Liu

Master of Science in Engineering Sciences (Mechanical Engineering)

University of California San Diego, 2021

Professor Jan Kleissl, Chair

Battery Energy Storage Systems (BESS) are often used for demand charge reduction through monthly peak shaving. The effect of two temporal resolutions, 15-min and 1-hour, on peak shaving is compared across a battery ratings space defined by power capacity and energy capacity of the battery. Based on the 15-min load of a particular day, a critical power and critical energy can be defined, yielding a critical point in the power-energy space. A linear program of the system optimizes the peak of the net load and the associated demand charge assuming perfect forecasts. Based on the difference of demand

charge (DODC) across the two load profiles at high and low temporal resolution for a real building, the battery rating space is divided into three different regions: optimal region, power-constrained region, and energy-constrained region, which can be identified by the critical power (CP) and critical energy (CE) derived from the load profile. As the conclusion shows, the DODC in the power-constrained and energy-constrained regions is explained by the averaging operation and the load sequence at high resolution. In the power-constrained region of the battery rating space, the difference between the original 15 min peak and the 1 hour average peak persists in the optimized net load until the battery power capacity is sufficiently large. In the energy-constrained region, averaging may change the peak period duration, which depends on the sub-hourly sequence of the original load data. Through artificial load data and reordering of real load data, we demonstrate that the sequence effect causes energy-constrained batteries to underestimate peak shaving and demand charge reduction.

Chapter 1

Introduction

Battery Energy Storage Systems (BESS) are critical to demand-side management for power end-users in microgrids, while also mitigating the challenges caused by uncertainty of renewable energy generation. BESS have become a popular solution for electricity cost reduction in commercial buildings through peak demand reduction and an associated reduction in demand charges. Largely owed to progress in technology and manufacturing in the last 5 years, the BESS costs have decreased dramatically. With many countries aiming to achieve sustainable power grids and reductions in carbon emissions, it is anticipated that BESS will be widely implemented in the near future.

There are two primary categories of existing BESS research: (i) utility side or "in front of the meter" applications and (ii) demand side or "behind the meter" applications [1]. In utility side applications, BESS can provide grid services to power systems with high levels of renewable penetration to decrease intermittency and disturbances [2, 3]. However, this paper targets demand side applications. Peak demand shaving of BESS is a

popular application in demand side management (DSM). Most commercial and industrial end-users are charged two components in electricity billing, energy charges and demand charges. Energy charges are based on the total energy (kWh) consumed while demand charges are a function of the peak demand in any 15-minute period of the billing cycle (typically one month). Through appropriate scheduling of charging and discharging (i.e., a battery dispatch strategy), BESS can reduce the peak demand and, thus, achieve economic savings[4]. To reach these goals, building and microgrid optimization typically requires forecasts of both renewable generation and electricity demand or load. For example, minimizing the annual energy cost by implementing mixed-integer linear programming (MILP), the DER-CAM model elucidated the drivers for adoption of BESS [4]. REopt evaluates economic viability, identifies system sizes of grid connected PV, wind and battery systems, and provides an optimal BESS dispatch strategy.

Battery dispatch scheduling is sensitive to the time resolution of the load profiles. Most analyses on temporal resolution use residential load profiles but do not consider minimizing demand charges or load peaks. Wright et al. [5] analyzed load averaging effects on import and export proportion of on-site generation for residential load with intervals ranging from 1 to 30 min. Longer averaging was unable to capture short-term peaks. Cao & Siren [6] analyzed the error of on-site production and demand matching capability as a function of time step size, which indicated the relationship between on-site generation of PV and load demand. Coarser resolutions overestimated the matching capability because the load variability decreased with averaging. A BESS reduced matching errors significantly due to the ability to flatten long sharp spikes. Beck et al. [7] assessed the effect of temporal

resolution of PV generation and electrical load profiles, comparing the self-consumption rate and optimal sizing of PV and PV+Battery (PVB) system from the optimal results of a MILP model based on resolutions ranging from 10 s to 60 min. A temporal resolution of 60 min was found to be sufficient for sizing both the PV and PVB systems. Especially for PVB, the influence of time resolution was negligible. Stenzel et al. [8] analyzed the impact of time resolution on self-consumption rates by PV BESS simulation model. Self-consumption was estimated incorrectly for longer averaging time due to smoothing, and thus lead to an overestimation of the cost-savings from PVB. Burgio et al. [9] studied the impact of data averaging on PVB system economics considering PVB system size. The temporal resolution did not affect the PVB sizing. However, a time resolution of 60-min caused a substantial under-estimation (up to 39%) of the peak load, as compared to a 3-min resolution.

Most of the research on the effect of temporal resolution targets self-consumption or self-sufficiency, which has been motivated by renewable feed-in policies (e.g., EEG in Germany). Self-consumption is overestimated at low time resolution, as it does not capture the high-frequency variation of the load and solar profiles. However, BESS peak shaving has not been examined as a function of temporal resolution. In other words, the effect of temporal resolution on demand charge reduction via optimal BESS dispatch scheduling needs to be analyzed. Per Burgio [9], peak loads of PVB system will be underestimated for low temporal resolution, but the reasons behind such errors have not yet been related to BESS properties.

The gaps in the literature are addressed by examining the difference between optimal

demand charges (viz the net load peak) achieved by BESS dispatch scheduling based on load profiles for two common temporal resolutions, 15 min and 1 hour. The 15 min interval is used by most utilities for customer metering, while the 1 hour interval is a more common resolution of solar resource data and typically applied in optimization models to reduce computational cost. We establish regimes of BESS benefits within the BESS power-energy rating space based on several pivotal indicators. A critical point separates the space into three regions: (i) power-constrained, (ii) energy-constrained, and (iii) optimal region. The magnitude and trends of the differences in optimization results at the two temporal resolutions are linked to the regions of the BESS space.

The rest of the paper is organized as follows: Section 2 reviews the methodology and mathematical assumptions, Section 3 presents the results, and Section 4 will provide conclusions and future directions.

Chapter 2

Methodology

2.1 Linear Programming Optimization

To focus on analyzing the effect of temporal resolutions, a simple energy system is adopted. Our system contains three main components: (i) the utility grid, (ii) the load, and (iii) a BESS with adjustable parameters (Fig. 2.1). All electronic interfaces are assumed to be 100% efficient. To study the economic savings of the behind-the-meter BESS, the meter net load given by P_g is recorded. P_g measures electricity imported from the utility resulting from the original load, l, offset by the negative or positive power compensation from the BESS. Without loss of generality, the load in this example is a true building load. But the same method can be applied for any time series, such as a net load resulting from summation of actual load and PV generators. Specifically, we are interested in the peak net load that determines the demand charge.

The optimization model is convex optimization problem, which is formulated in discrete

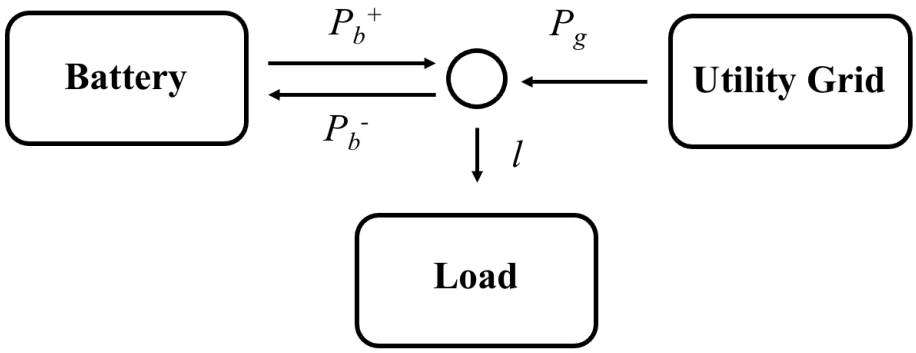

Figure 2.1: Schematic of the power system including a BESS, load, and utility grid with power flows.

time with time step size, Δt, determined by the temporal resolution of the load profile. The system energy conversion and transmission is perfectly efficient. BESS response is assumed to be instantaneous, such that the charging/discharging dispatch is "on demand". Given that the response time of Lithium-ion type batteries is on the order of milliseconds (i.e. much smaller than the time interval), this assumption is justified [1]. The charging/discharging power of BESS, P_b (kW), is only limited by the nominal power capacity, c_p (kW), and energy capacity, c_e (kWh). The convex optimization problem minimizes an objective function obj as:

$$\min \quad obj = d \times \max(P_g) + \epsilon \times \sum_{n=0}^{N} |P_b^n|, \tag{2.1}$$

where d is the demand charge rate, ϵ is a penalty factor, N is the number of time steps, and n is the time index. The first term in the objective function measures the maximum

net load, which is called optimal peak, OP (kW):

$$OP = \max(P_g) \tag{2.2}$$

The demand charge rate, $d = 20.62$ \$/kW, is included as a multiplier to demonstrate the economics of reducing the optimal peak; d is obtained from the AL-TOU rate schedule for >500 kW demand by the local utility San Diego Gas & Electric (SDG&E). This rate does not affect the generality of the results but is included for illustrative purposes. Thus, the optimal demand charge (ODC) is given by:

$$ODC = d \times \max(P_g) = d \times OP \tag{2.3}$$

The second term is a penalty for charging/discharging power decisions. Of the many possible solutions with equal objective function, the penalty term ensures that the solution with the least battery activity is selected. By multiplying in a small coefficient, $\epsilon = 10^{-6}$, the convex optimization model diminishes the oscillation of P_b^n while simultaneously preserving the ODC, because the first term has a much heavier weight than this penalty term.

The constraints are:

$$\text{Energy balance:} \qquad P_g^n + P_b^n = l^n, \qquad \forall n \in N \tag{2.4a}$$

$$\text{Power capacity:} \qquad -c_p \leqslant P_b^n \leqslant c_p, \qquad \forall n \in N \tag{2.4b}$$

$$\text{State of charge:} \quad SOC^{n+1} = SOC^n - \frac{P_b^n \times \Delta t}{c_e}, \forall n \in N \tag{2.4c}$$

$$\text{Initial state:} \qquad SOC^1 = SOC^{end} = 0.5 \tag{2.4d}$$

where SOC is the state of charge of the BESS. Equation (2.4a) requires that, at each time step, net load supplied by the grid and the BESS must equal the load demand. According to (2.4b), the power from the BESS is constrained by the power capacity; $P_b^n > 0$ indicates discharging the BESS, and $P_b^n < 0$ indicates charging. While the BESS is charging or discharging, SOC must be consistent with the BESS dispatch schedule as stipulated in the (2.4c). Following a common optimization scheme for daily time horizons, the BESS is further constrained to be half charged at both the beginning and end of the day. Applying this initial setting by (2.4d), savings through energy sales are avoided as the net charging/discharging energy after the simulation period, T, is zero. The optimization model is built using CVX on MATLAB with the MOSEK solver.

2.2 Load data and difference of optimal demand charge (DODC)

The load data collected on October 7, 13, and 24 in 2019 from the Police building on the campus of the University of California, San Diego (UCSD) is analyzed. The data show typical variations for commercial buildings but does not limit the generality of the LP model. Although the demand charge is usually measured in billing cycles of one month, this study examines only one day at a time for illustrative purposes (i.e., $T = 24$ hours). The load data on October 7, 13, and 24 are chosen as inputs. The optimization results are discussed and compared in Section 3.

We consider two temporal resolutions of the input data: 15 min and 1 hour (i.e.,

60 min). Since the load is measured as interval data of 15-min by the real SDG&E meter, 15 min is defined as the reference temporal resolution. On the other hand, many data sets, analyses, or optimization models for peak shaving are based on a 1 hour resolution (e.g., REopt). The low-resolution profile is derived by taking the average of four high-resolution time steps (Fig. 2.2). The number of battery dispatch decisions (i.e. number of time steps), N, along a same scheduling horizon, T for the 15 min resolution is 4 times that of the 1 hour resolution. For optimizing dispatch scheduling of one day, where $T = 24$ hours, the decision numbers are given by:

$$N_{1-hour} = \frac{T}{\Delta t_{1-hour}} = 24, \quad \text{and}$$
$$N_{15-min} = \frac{T}{\Delta t_{15-min}} = 96$$

The 1 hour averaged load data may result in a different objective function value compared to the original load profile, which subsequently leads to a different optimal peak and a different optimal demand charge. This deviation is defined as the difference of demand charge, DODC:

$$DODC = ODC_{15-min} - ODC_{1-hour} \tag{2.5}$$

where ODC_{15-min} and ODC_{1-hour} are the optimal demand charge achieved using the same battery and adopting the load profiles with 15 min and 1 hour time resolution, respectively. DODC indicates the peak shaving error caused by applying a load with coarser (lower) temporal resolution as compared to one with a higher temporal resolution. DODC is hypothesized to depend on the BESS capacities – namely, power capacity, c_p, and energy capacity, c_e.

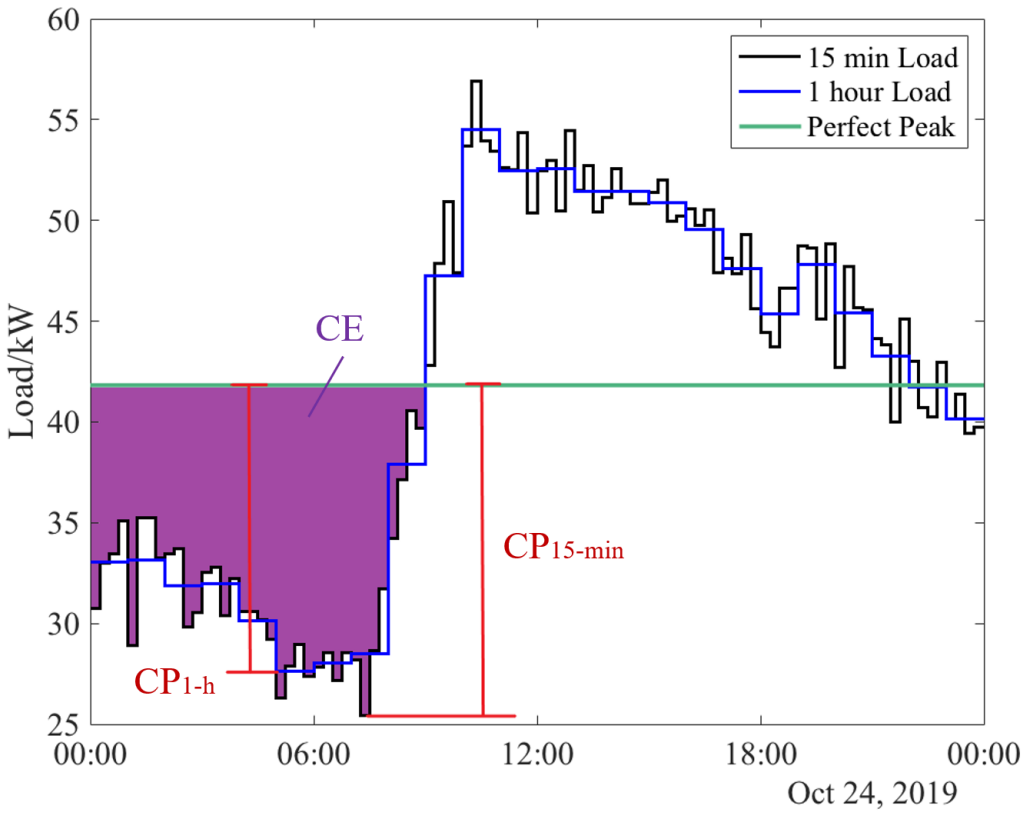

Figure 2.2: 15 min and 1 hour temporal resolution load profiles, along with the perfect peak, on October 24. The maximum 15 min load occurs from 10:15-10:30 h at 56.89 kW, while the perfect peak is 41.83 kW.

2.3 Battery space analysis

Given a specific load profile, the OP and corresponding ODC are determined by the BESS capacities. Due to human activity and equipment schedules, the load of a building varies based on the time of day. Generally, there may be one or several local peaks in the load profile. During the peak period(s), the BESS responds to supply the load to limit grid imports once the power demand exceeds the optimal peak. Since the SOC at

the end of the day is constrained to be the same value as the beginning of the day, the net electricity energy discharged from the BESS must be zero. Therefore, the BESS must recharge after each peak period. Hence, the BESS is able to shift demand, and its capacity ratings determine how much power and energy it can move. In other words, the demand peak reduction depends on the capacity of the BESS.

Several indicators characterize the load profile. The perfect peak, PP (kW), is the average power of the daily load:

$$PP = \frac{\sum_t^T l^t}{T} \tag{2.6}$$

A reduction of the load peak to the PP can only be achieved by a sufficiently large BESS. For a particular load profile, the battery will have an ideal c_p and c_e, such that any larger capacity will not lower the optimal peak. These ideal capacities are henceforth defined as critical capacities— critical power, CP (kW), and critical energy, CE (kWh):

$$CP = \max |l^t - PP|, \quad \text{and} \tag{2.7a}$$

$$CE = 2 \times \max |\sum_1^t [(l^t - PP) \times \Delta t]| \tag{2.7b}$$

CP measures the maximum distance from the load to the PP at each time stepBecause load profiles tend to be positively skewed, the positive maximum distance from the load is expected to be larger than the negative distance, while negative maximum charging power is still possible to be larger as shown in Fig 2.2. CP_{15-min} and CP_{1-hour}, describe the critical power for the 15 min and 1 hour temporal resolutions, respectively. It is intuitive that the distance between the PP and extreme points in the 1 hour load is smaller than or equal to that of the 15 min load; thus, CP_{1-hour} is smaller than or equal to CP_{15-min}

(as depicted in Fig. 2.2). The overall CP is defined as CP_{15-min}, as derived from 15 min load:

$$CP = CP_{15-min} \tag{2.8}$$

CE takes the maximum absolute value of the cumulative sum of the distance from the 15 min load to the optimal peak for all time steps. This measures the minimum BESS energy capacity required to guarantee achieving the PP.

As the BESS capacities determine the OP for a particular load, it is necessary to examine the variation of the DODC with BESS energy and power capacities. To measure both the power and energy capacities, the battery ratings space has two dimensions (Fig. 2.3) The critical point is found at the intersection of the CP and CE lines. Note that the CP and CE change from day to day.To derive the DODC across the whole battery rating space, each BESS candidate (i.e., every point in this battery space) is chosen to be the input to the model given the load profile of a particular day. The DODC is then calculated based on the optimization results of net load for both the 15 min and 1 hour temporal resolutions.

Based on the critical point and critical lines, the battery rating space is divided into four regions O, P, E, and S in Fig. 2.3. BESS's larger than the critical point in both power and energy (optimal region "O") will have a DODC of exactly zero. Once the BESS capacity reaches the critical capacity, load at any temporal resolution can be reshaped to the optimal result (the PP) and the additional battery capacity is not used. Hence, region (O) is regarded as the "optimal region," where the ODC for the load in both temporal

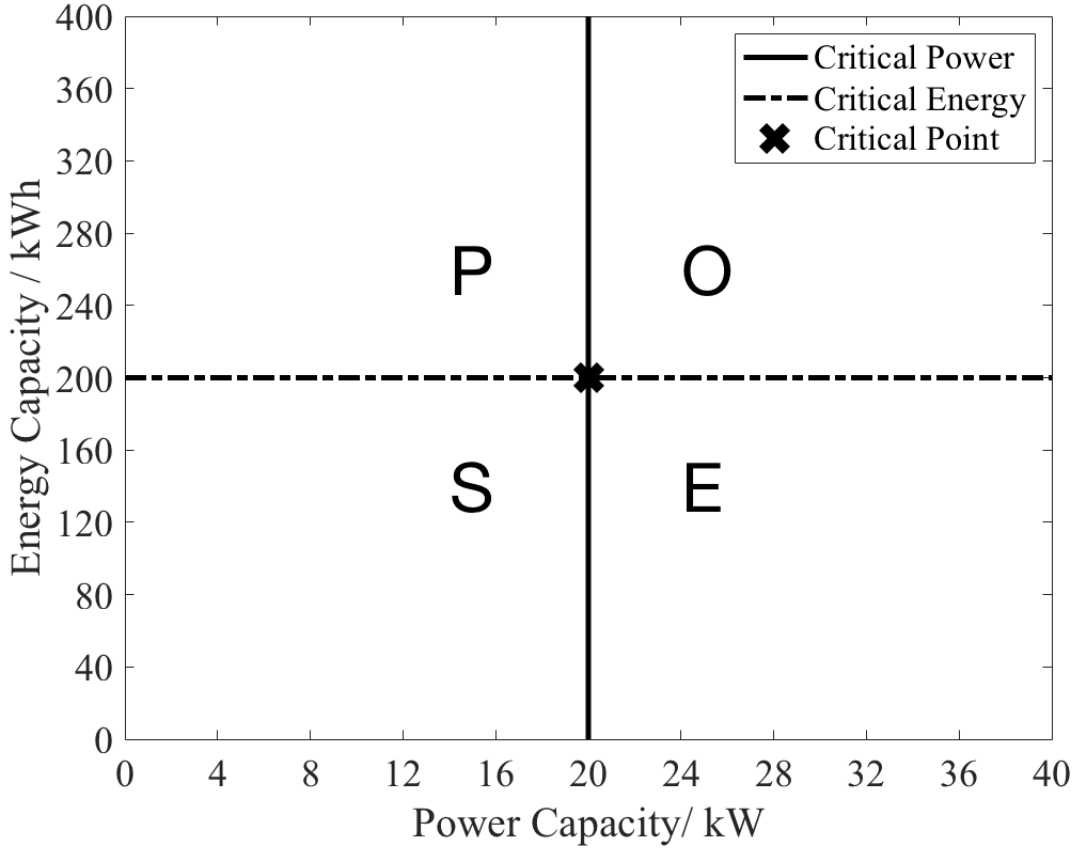

Figure 2.3: Conceptual diagram of a typical battery ratings space. The quadrants are marked as "optimal" (O), "power-constrained" (P), "energy constrained" (E), and "small" (S).

resolutions are the same. BESS's with either power or energy capacity smaller than the critical point will not be able to reduce the peak down to the PP for load profiles in both resolutions. Then, the two OP's will differ from each other, and the DODC will not equal zero. In region (P), insufficient BESS power capacity restricts peak shaving ability, while the energy capacity is sufficient. In region (E), BESS's with sufficient power capacity but insufficient energy capacity are charted. In region (E), if the energy capacity is fixed while

power capacity is increased gradually, the two OP's and ODC's will not change because the energy capacity limits the performance of demand shaving. Therefore, regions (P) and (E) are the "power-constrained region" and "energy-constrained region," respectively. In region (S), "small" BESS's are constrained in both energy and power ratings, and the DODC will vary depending on the BESS capacities and load profile.

Chapter 3

Results and Discussion

3.1 Overview

Fig. 3.1a shows an overview of the DODC across the battery space derived from the load on October 24. The ODC for the 15 min and 1 hour loads is shown respectively in Fig. 3.1b and Fig. 3.1c. As defined above, the DODC at each point in the battery space is derived from taking the difference of the corresponding two ODC's. Thus, the Fig. 3.1a charts the "difference" between Fig. 3.1b and Fig. 3.1c. From the two ODC plots, it is confirmed that the ODC is inversely proportional to BESS capacity. The flattened region, where power and energy capacity become large, indicates that PP can be achieved after the critical point for both load profiles. Thus, the value of ideal demand charge is the same (i.e., \$862.40). For ODC's of 15-min resolution, the reduction of ODC at the PP is \$211.60, or 19.7% of the maximum load profile value, \$1074. This significant reduction supports the potential of BESS to make significant economic savings in demand charge

management behind the meter.

The distribution of DODC in Fig. 3.1a is consistent with our conjectures about the optimal, power-constrained, and energy-constrained regions in Fig. 2.3. Fig. 3.1a also displays an example of the DODC behavior for small BESS's, as given by Region (S) in Fig. 2.3. These findings confirm that the 1 hour load profile will overestimate peak shaving, as the DODC values are non-negative across the battery ratings space. In the optimal region, DODC is zero as expected. In the power-constrained region, DODC is independent of energy capacity; in the energy-constrained region, DODC is independent of power capacity. Region (S) is divided into two parts that resemble their neighbors P and E, allowing the battery space to be simplified into three P, E, and O regions (Fig. 3.2). While the pattern in Fig. 3.1 is derived from the load profile of October 24, the generality is confirmed by other days. The battery space consisting of the critical point and three characteristic regions is the characteristic pattern of the DODC for any load profile.

The optimal region represents the PP pattern; on the other hand, the two capacity-constrained regions still require further discussion. In Section 3.2, the power-constrained region is discussed, and the peak shaving by load averaging is quantified. In Section 3.3, complex situations for the energy-constrained region are discussed, including a comparative analysis of the DODC results from different days. Section 3.3 also elucidates how the sequencing of 15 min load during the peak period affects the boundaries between the regions.

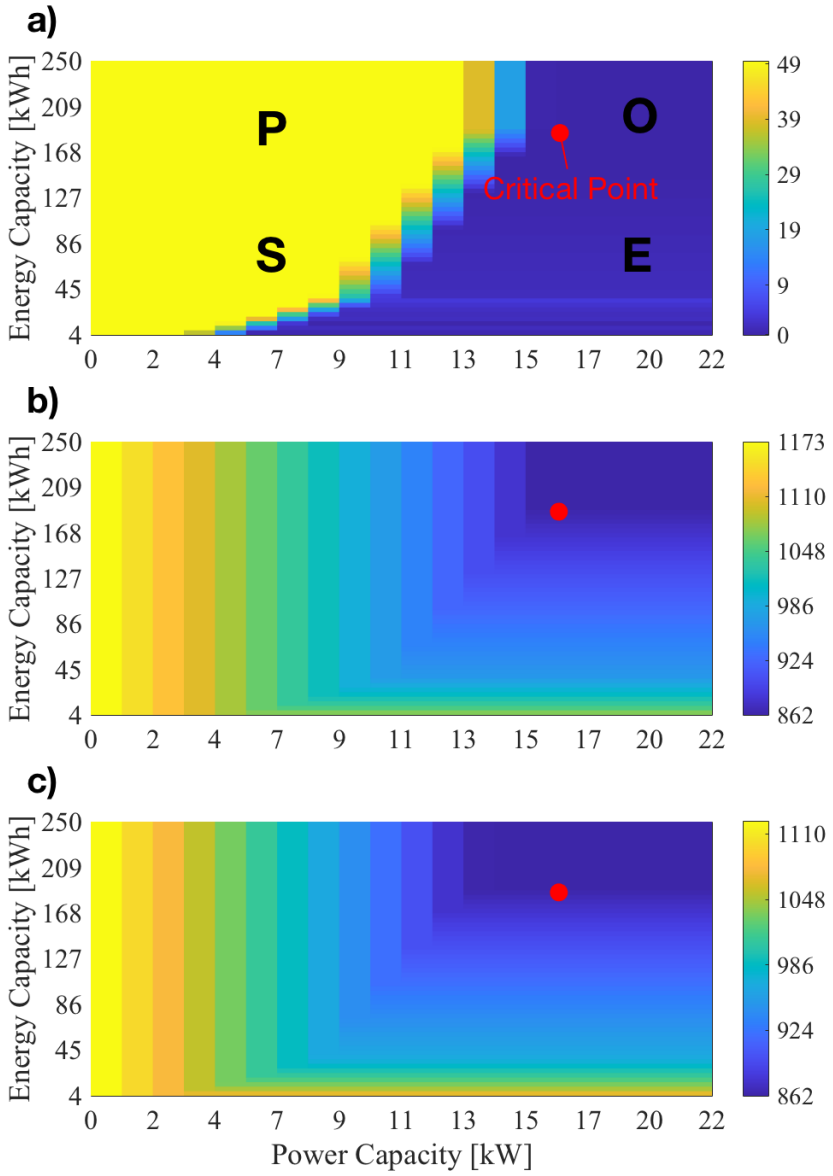

Figure 3.1: Demand charge metrics ($, color) for October 24 as a function of power and energy capacity: (a) DODC, (b) ODC of 15 min load, and (c) ODC of 1 hour load. (a) is the difference between (b) and (c). The red circle shows the critical point. The four quadrants in Fig. 2.3 is marked around the critical point in (a).

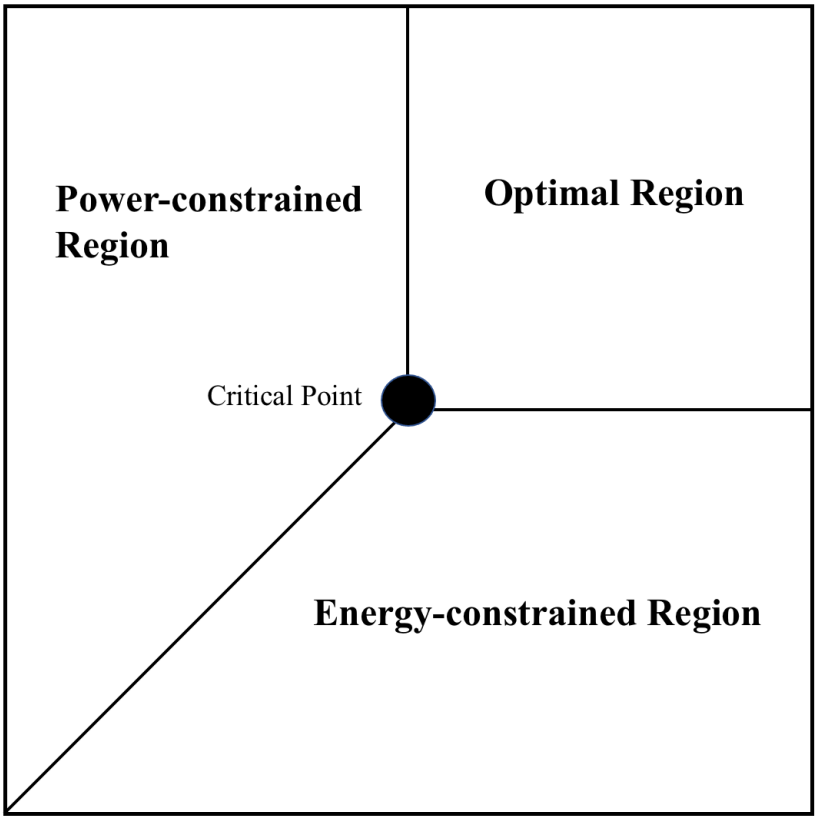

Figure 3.2: Simplified three-region battery space.

3.2 Power-constrained Region

The power-constrained region is analyzed based on a selected fixed energy capacity, where the corresponding ODC of each load is then extracted along with the corresponding DODC (Fig. 3.3). To eliminate energy capacity constraints, the fixed energy capacity value should be larger than the CE of the load profile, which is 188.2 kWh for October 24. For a fixed energy capacity of 224.9 kWh, the DODC, the $ODC_{15\text{-min}}$ and the $ODC_{1\text{-hour}}$ are shown in Fig. 3.3. In Fig. 3.3, horizontal slices of the battery ratings space at the fixed energy capacity are plotted together for the 15 min and 1 hour temporal resolution: the

left side, P, represents the power-constrained region, while the right side, O, represents the optimal region. The two sides are split by the CP. As the battery power capacity increases, $ODC_{15\text{-min}}$ and $ODC_{1\text{-hour}}$, decrease linearly and in parallel with a fixed difference of \$49.60, starting from \$1124 and \$1074 respectively. This trend remains until the power capacity reaches the CP, after which both ODC's settle at the same level. The DODC is constant until the power capacity reaches 12.47 kW, where DODC falls rapidly before settling at zero for 16.4 kW power capacity.

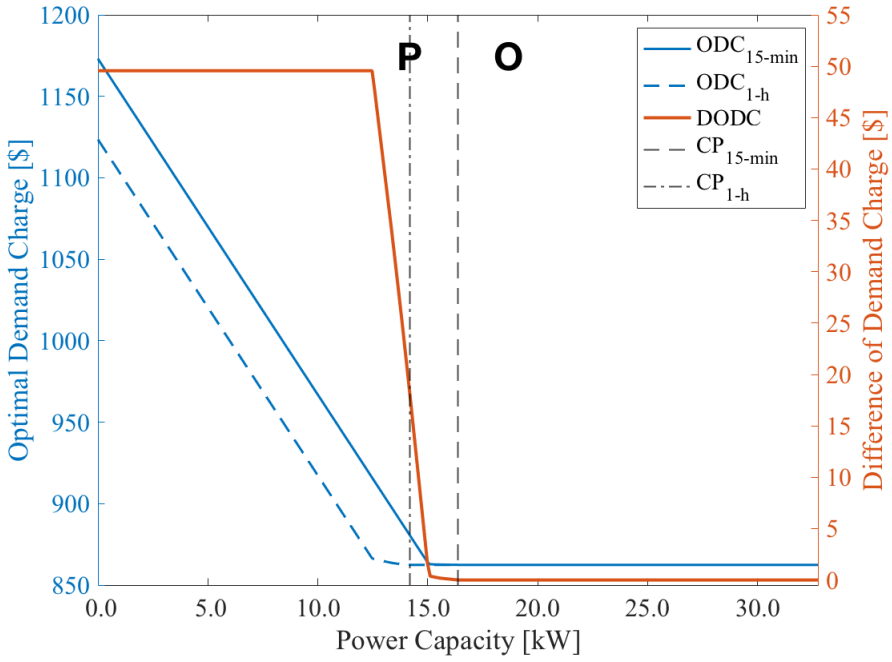

Figure 3.3: DODC, $ODC_{15\text{-min}}$, and $ODC_{1\text{-hour}}$ on Oct 24 at a fixed BESS energy capacity of 224.9 kWh.

The ODC in the power-constrained region is affected by time averaging operation of the load from high-resolution (15 min) to low-resolution (1 hour). The constant DODC of

$49.60 for power ratings smaller than the transient zone in Fig. 3.3 results from

$$(ML_{15-min} - ML_{1-hour}) \times d = \$49.60 \tag{3.1}$$

where $ML_{15\text{-}min}$ (56.9kW) and $ML_{1\text{-}hour}$ (54.5kW) are the maximum load demand of October 24 for the two time resolutions. For example, Fig. 3.4a displays the loads and net loads as optimized by a randomly selected BESS from the power-constrained region. $ML_{15\text{-}min}$= 47.5 kW occurs at 10:15-10:30 h while $ML_{1\text{-}hour}$= 45.1 kW occurs at 10:00-11:00 h. The difference of 2.4 kW is constant throughout the peak period, resulting in DODC=$49.60 for the day.

The sharp drop in DODC occurs around the CP of each load for both temporal resolutions. Hence, CP adequately describes the transient zone between the power-constrained and the optimal regions. The beginning and end of the transient zone, 12.47 kW and 16.4 kW, are close to the CP of the 1 hour and 15 min load, $CP_{1\text{-hour}}$=14.2 kW and $CP_{15\text{-min}}$=16.4 kW for October 24. This advanced start can be explained by the variation patter of $ODC_{1\text{-hour}}$, as it falls close to the PP quickly before 12.47 kW and then keep decreasing in a extremely small speed until $CP_{1\text{-hour}}$. The same phenomenon can also be observed in $ODC_{15\text{-min}}$, and it results in the slowly decreasing of DODC after 15 kW. The difference of the two CP's is caused by load averaging. Fig. 3.4b displays the optimization results of a BESS with capacity of c_p=$CP_{1\text{-hour}}$ and fixed energy capacity. With a power capacity of $CP_{1\text{-hour}}$, the 1-hour net load becomes flat and equal to the PP of 41.8 kW. However, the $CP_{1\text{-hour}}$ BESS is unable to completely flatten the 15 min load timeseries, resulting in a net load peak of 42.7 kW during 10:15-10:30 h. The 0.9 kW increase over

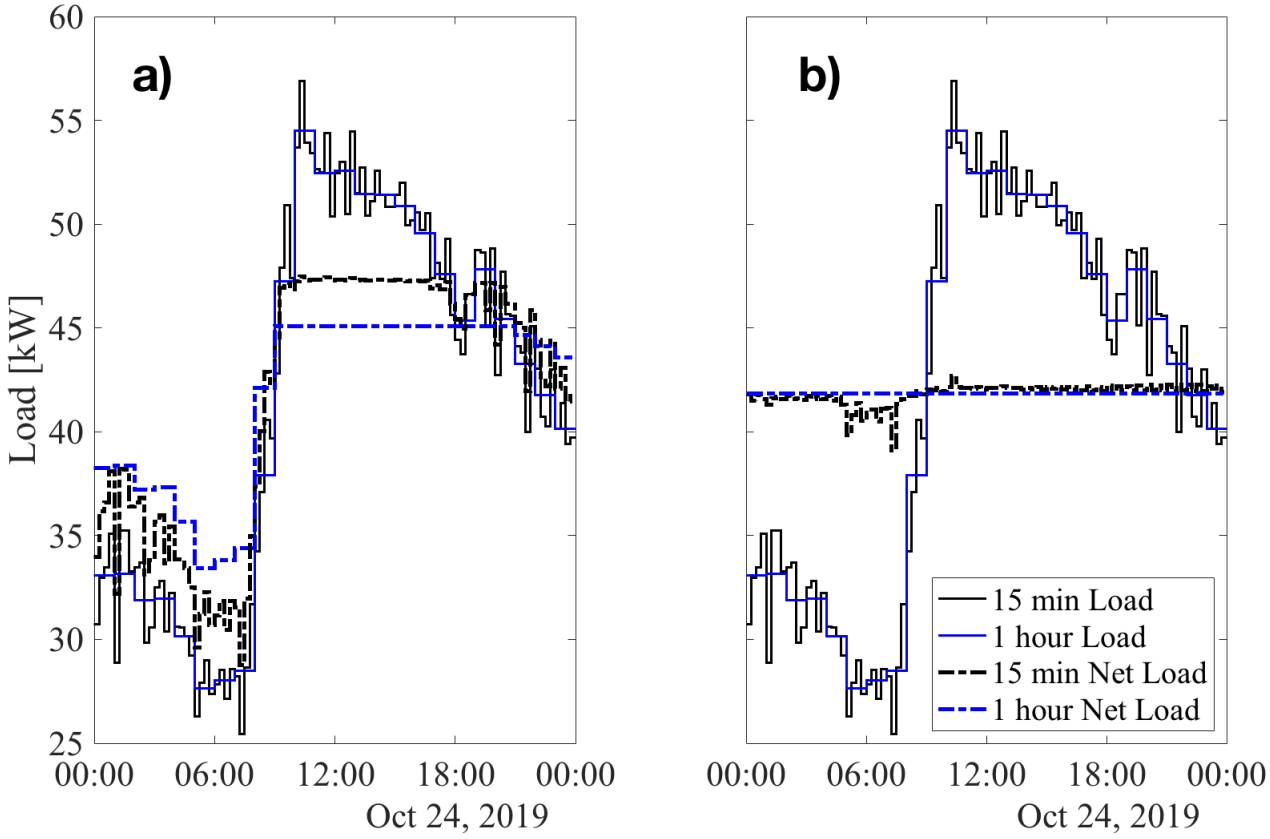

Figure 3.4: 15-min and 1-hour load on October 24 and net load optimized by the following BESS: a) 9.4 kW, 224.9 kWh; b) 14.2 kW (=$CP_{1\text{-}hour}$) and 224.9 kWh.

PP results in a DODC=\$18.60 in Fig. 3.3.

Based on analyzing time series at two temporal resolutions, the transient zone is spanned by the CP's from the two temporal resolutions, and the constant DODC in the power-constrained region can be calculated. Given a BESS of sufficiently large energy capacity, the peak shaving depends solely on two factors: the peak demand (maximum load in units kW) and the power capacity of the BESS. The energy capacity will not constrain the peak shaving effect, but the power capacity of the BESS will be fully utilized at the

peak demand interval. The original peak difference between the two load profiles is maintained, as the limited power capacity of the BESS is unable to reduce the peak demand to the PP line. Even when the energy capacity is lower than the critical point (as in region S in Fig. 2.3), there will be a range (i.e., the lower power-constrained part of region S in Fig. 3.2) in which the peak shaving is limited by the power capacity, thus maintaining the original peak difference.

3.3 Energy-constrained Region

3.3.1 Three example days: Overview

To analyze the DODC in the energy-constrained region, the power capacity is fixed at the CP. Fig. 3.5 presents the variation of the $ODC_{15\text{-min}}$, $ODC_{1\text{-hour}}$, and the corresponding DODC at the CP of three different days: Oct 7 (CP = 10.2 kW), Oct 13 (CP = 16.4 kW), and Oct 24 (CP = 12.0 kW). Selecting a fixed power capacity of CP eliminates the potential influence of insufficient power, ensuring that the effect of constrained energy capacity can be analyzed in isolation. In Fig. 3.5, the left part, E, represents the energy-constrained region, while the right part, O, is the optimal region. The DODC at zero energy capacity is the same value as in the power-constrained region, but this DODC value cannot be maintained as the energy capacity increases. The ODC's at both resolutions are noticeably closer to each other, as compared to those in the power-constrained region in Fig. 3.3. Thus, the DODC magnitude is also much smaller except for trivial points close to zero capacity. However, the variation of the DODC in the energy-constrained region is

more complex and irregular than in the power-constrained region.

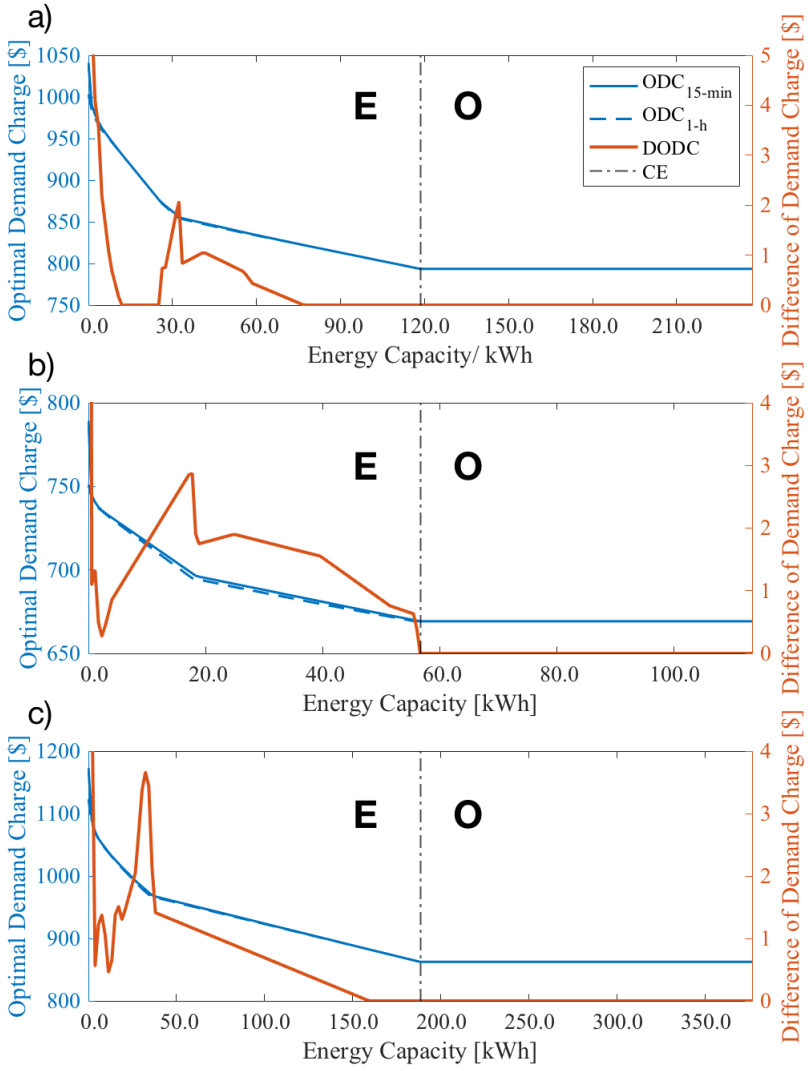

Figure 3.5: The DODC corresponding to the critical power capacity in the battery ratings space of a) Oct 7, b) Oct 13, and c) Oct 24. O represents the optimal region, and E represents the energy-constrained region. The vertical dashed line represents the critical energy (CE).

The energy-constrained regions of Oct 7 and Oct 24 shows a significant feature: the

DODC may be zero at some energy capacity smaller than CE. For Oct 24, DODC= 0 from 169.9 kWh to CE (Fig. 3.5c), and for Oct 7, DODC= 0 at 18.85 kWh and from 84.45 kWh to its CE (Fig. 3.5a). However, this feature is inconclusive and irregular, as DODC$\neq$ 0 in the energy-constrained region for Oct 13 and the distributions of zero DODC for Oct 7 and 24 differ greatly. We speculate that the reason could be a change in the peak period duration of some load profiles after time-averaging. For other load profiles, when the averaging does not change the peak period duration, DODC= 0 as expected. We test this hypothesis which we refer to as "sequence effect" through artificial load profiles and then verify the conclusion using real data from Oct 7.

3.3.2 Artificial load and sequencing

To illustrate the impact of the load sequence on DODC in the 15-min profile, a regular U-shaped load with a flat peak demand from 11:00 to 17:00 h is employed. In Fig. 3.6, the two load profiles at 15 min are identical except that they differ slightly in the beginning of the peak period (i.e., 10:00–11:00 h). But the hourly averages are identical. As shown in Table 1, the power demands within this particular hour in the two 15-min U-loads have the same values but are arranged in a different order; in other words, the sequence differs.

Since the three U-shaped loads (i.e., the two 15 min profiles and the 1 hour profile) have identical peak loads, the net load peak is not affected by the power capacity of the BESS. However, the 15 min load sequence at the start of the load peak (e.g., 10:00-11:00 h) changes the shape of the load during the peak period. An energy-constrained BESS, with power capacity of 25 kW and energy capacity of 45 kWh, is selected for the

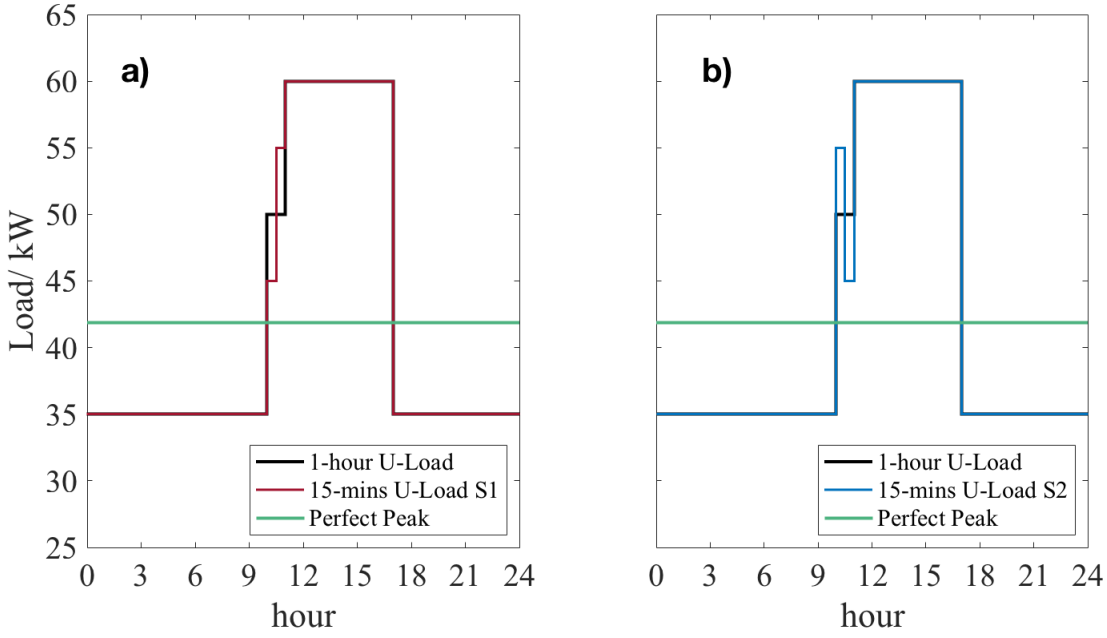

Figure 3.6: Artificial load profiles at 15 min and averaged to 1 hour: a) Sequence 1, and b) Sequence 2

Table 3.1: Data of the artificial load time series shown in Fig. 3.6. The three load profiles share the same CP of 20.2 kW and the same CE of 195.8 kWh

	Load Profile / kW			
	0:00-10:00	10:00-11:00	11:00-17:00	17:00-24:00
1-hour	35	50,50,50,50	60	35
15-min Sequence 1	35	45,45,55,55	60	35
15-min Sequence 2	35	55,55,45,45	60	35

net load peak optimization (Fig. 3.7). The OP is nearly the same: the CP for Sequence 1 (52.69 kW) is 0.49 kW higher than for Sequence 2 (CP= 52.50 kW) and for the 1-hour

average (CP= 52.50 kW). Though this difference is small, it is of fundamental interest because the DODC changes from zero to non-zero as a result of a small modification from Sequence 2 to Sequence 1.

As the BESS energy is sized to achieve an optimal net load between 50 kW and 55 kW, the starting point of the peak period of the 1 hour load and Sequence 2 is at 11:00 h, while the counterpart in Sequence 1 is at 10:30 h instead due to its step-shaped peak demand period. The peak demand period from 10:30 to 17:00 h of Sequence 1 then contains a part of the load in 10:30-11:00 h. Therefore, a BESS with a limited energy capacity can achieve greater peak shaving and a lower net load peak for the 1 hour averaged load than for Sequence 1. This difference in the start time of the peak period also manifests in the SOC plot, where the discharging period starts at 10:30 h for Sequence 1 but at 11:00 h for Sequence 2 and the 1 hour averaged load. On the other hand, Sequence 2 has a recharging period of 10:30-11:00 h, recovering the BESS after discharge from 10:00 to 10:30. This recovery more efficiently uses the limited energy capacity, as the net effect of the high-low load Sequence 2 in 10:00-11:00 h is the same as for the aggregated 1 hour U-load. Subsequently, the 1 hour Load and Sequence 2 have identical optimal peaks.

In summary, a difference in sequence in the 15 min load can affect the optimal net-load peaks. In this example, the 15 min sequence in the beginning of the peak period has a lower demand followed by a higher demand with an identical hourly average. The result is an increased optimal net-load peak, as compared to the corresponding 1 hour load. This occurs because the duration of the peak period is extended, and the integral between the target peak net load and the original load then contains more energy that cannot be

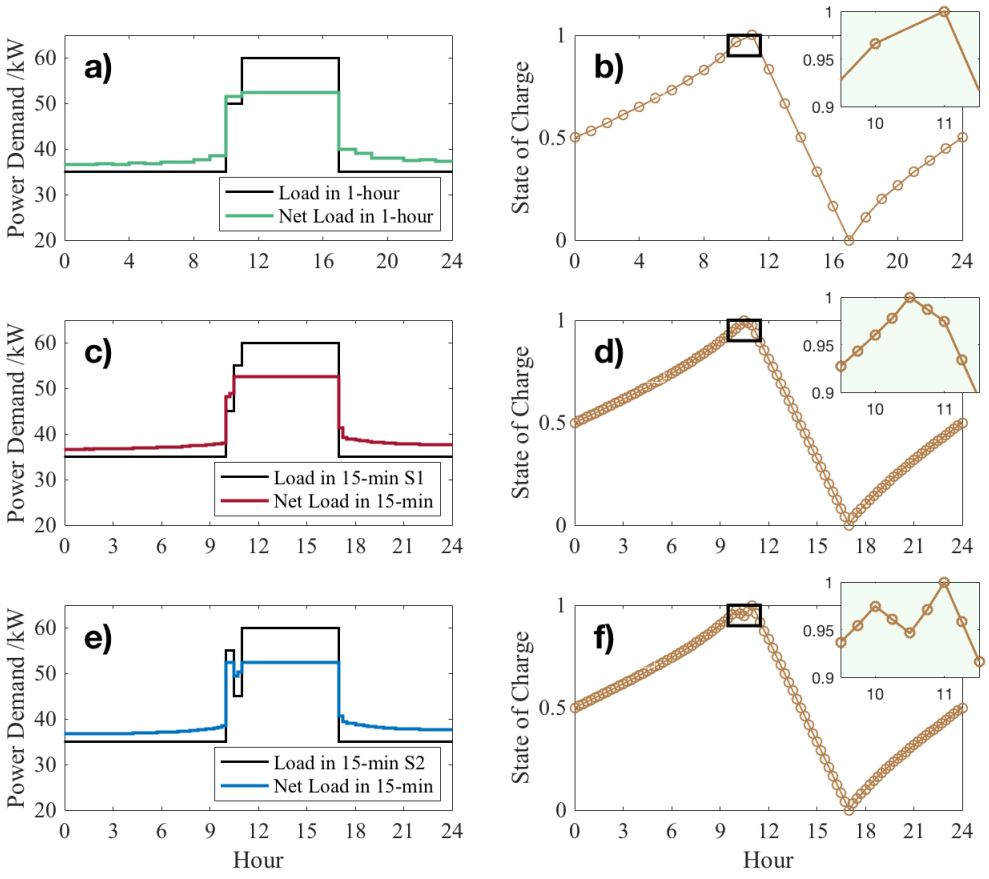

Figure 3.7: a) 1 hour U-shaped load and its net load optimized by an energy-constrained battery and its b) SOC. c, d) the load, net load and SOC of the 15 min load in Sequence 1. e, f) the load, net load and SOC of 15 min load in Sequence 2.

shaved by a battery with limited energy capacity. Note that the energy sequence during the original load peak period is irrelevant, as it does not extend the duration of the peak period. However, the energy sequence at the end of the peak period also affects the optimal peak; a decreasing trend in the 15 min energy sequence will increase the optimal peak, while an increasing trend will result in zero DODC.

3.3.3 Sequence Verification on Oct 7

To verify the energy sequence effect conclusions from the artificial data, a modified 15 min load from Oct 7 is designed and the corresponding battery space is studied. According to the original DODC results in Fig. 3.5 and the load in Fig. 3.8, for a small battery energy capacity the peak period before OP falls to 45 kW starts from 13:00-14:00 h and ends at 15:00-19:00 h. As the OP falls to 40 kW-45 kW, the peak period extends from around 9:00-12:00 h to after 18:00 h. Following the analysis in Section 3.3.2, we can achieve optimal net load peak equality between 15 min and 1 hour loads by re-ordering the energy sequence within these specified hours. During the beginning of the peak period, the four 15 min periods within each hour are reordered from largest to smallest and opposite sequencing is applied at the end of the peak period (see the Table A.1 in the Appendix for the numerical values). The modified version shares the same 1 hour average, CE capacity, and CP capacity as the original load. A slice across the energy-constrained region at CP based on the optimization result for the DODC across the battery power rating space of the modified Oct 7 load is shown in Fig. 3.9. The DODC in all energy-constrained regions are now zero (except when XXX is zero), supporting our hypothesis about the sequence effect.

As shown, averaging might affect the duration of the peak period based on the particular sequence of the load. Averaging can cover up the arrangement of energy sequence in the original 15 min load profile. Therefore, for energy-constrained BESS, averaging the load input data can result in an underestimation of ODC for the net load.

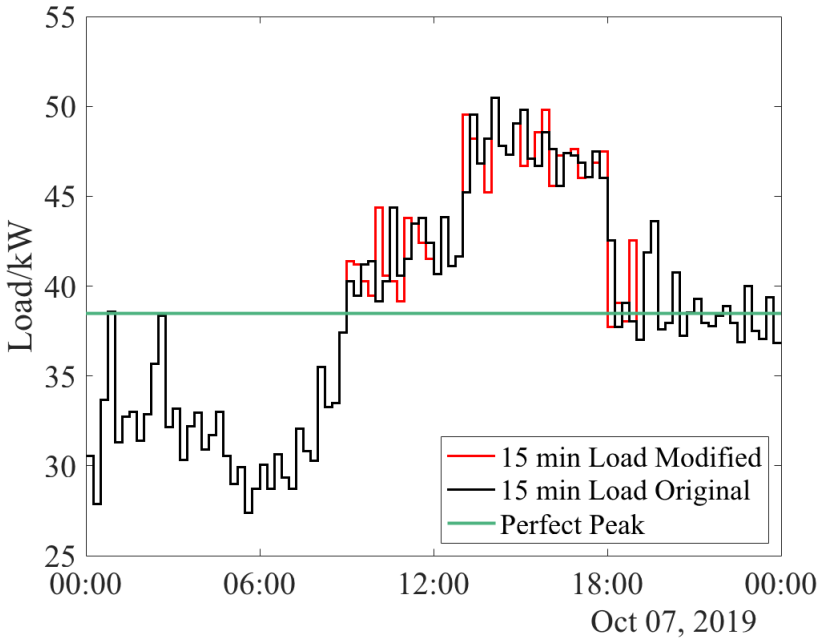

Figure 3.8: Original load profile on Oct 7 and the modified version with energy sequence changed in specific periods.

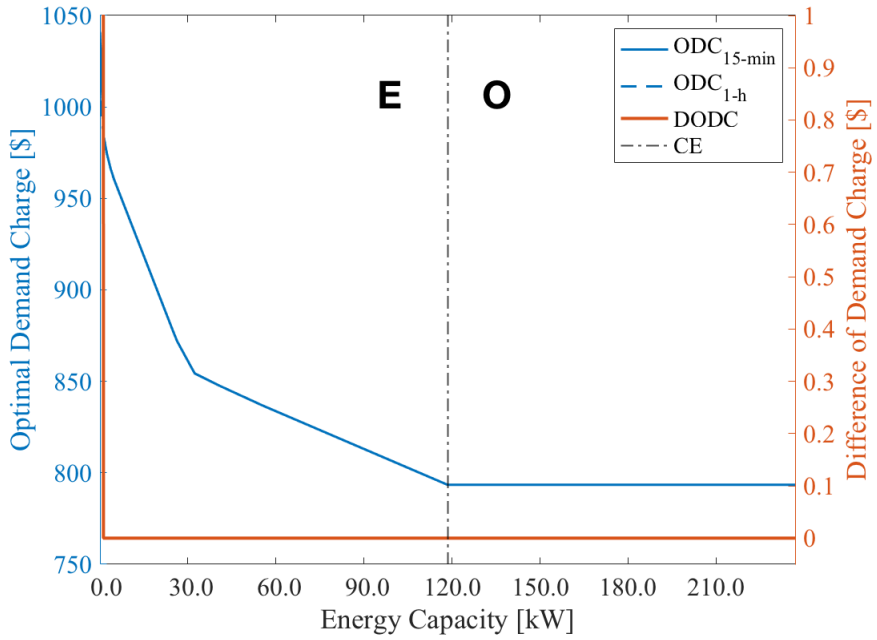

Figure 3.9: The DODC for the critical power capacity for the modified load of October 7. O represents the optimal region, and E represents the energy-constrained region. Compared to Fig. 3.5a, DODC is now zero in throughout except for zero energy capacity.

Chapter 4

Conclusions

The conclusions derived from the load data of the one-day period can be extrapolated for demand charge analysis of a month, or even a whole year. This is because the peak load of a time period longer than a single day varies based on the most challenging day(s) within the period (i.e., the days with largest critical power (CP) or critical energy (CE)). For load profiles with a "spiky" peak caused by short peak duration (i.e., high CP, low CE), the overestimation of optimal demand charge tends to be high for low-resolution load of a BESS in the power-constrained region. On the other hand, for load profiles with a "broad" peak (i.e., low CP, high CE), the error is more sensitive to batteries with limited energy capacity, and thus, the DODC in energy-constrained region tends to be more significant. If the type of peak (spiky versus broad) shifts during the year, then a BESS may be designed to be power-constrained during the broad months and energy-constrained during the spiky months. Demand charges are calculated monthly, meaning that annual results may then be a combination of power-constrained and energy-constrained characteristics.

In this paper, 15-min and 1-hour intervals are chosen for comparison as high- and low-resolution, respectively. However, the analysis and conclusions also apply for other temporal resolutions. The concept of partitioning the BESS ratings space offers a new perspective for the study BESS demand shaving as well as systems including on-site renewable generators at different temporal resolutions. The details of high-resolution profiles should be considered carefully in demand side management for a BESS with limited capacities. This is critical not only to capture high peak demand within a high-resolution sampling time step, but also for the energy sequence that indicates the order of power load. Choosing a BESS with a large capacities can offset the uncertainties from load resolution conversion in demand shaving estimation. This comprehensive study of the effect of temporal resolutions in peak shaving involves batteries of various scales, providing important insights in the intrinsic properties of load profiles and their relationship with BESS ratings. In turn, this research offers new insights in demand side management and BESS implementations for a more sustainable power grid.

The thesis is currently being prepared for submission for publication of the material. Liu, Shiyi; Silwal, Sushil; Kleissl, Jan. The thesis author was the primary investigator and author of this material.

Appendix A

Table A.1: The load data in specific hours of original 15-min load profile on Oct 7 and its modified version.

	Special Periods of 15-min Load Profile /kW							
	9:00-10:00	10:00-11:00	11:00-12:00	13:00-14:00	15:00-16:00	16:00-17:00	17:00-18:00	18:00-19:00
Original Load	40.27	39.15	41.53	45.23	49.82	47.61	46.85	42.52
	39.46	40.27	43.48	49.53	47.09	45.56	46.06	37.74
	41.22	44.39	43.79	46.81	46.70	47.39	47.47	39.05
	41.37	40.57	42.40	48.20	48.54	47.24	46.02	38.04
Modified Load	41.37	44.39	43.79	49.53	46.70	45.56	46.02	37.74
	41.22	40.57	43.48	48.20	47.09	47.24	46.06	39.05
	40.27	40.27	42.40	46.82	48.54	47.39	46.85	38.04
	39.46	39.15	41.53	45.23	49.82	47.61	47.47	42.52

References

[1] A. Nottrott, J. Kleissl, and B. Washom. Energy dispatch schedule optimization and cost benefit analysis for grid-connected, photovoltaic-battery storage systems. *Renewable Energy*, 55:230 – 240, 2013.

[2] Haisheng Chen, Thang Ngoc Cong, Wei Yang, Chunqing Tan, Yongliang Li, and Yulong Ding. Progress in electrical energy storage system: A critical review. *Progress in Natural Science: Materials International*, 19(3):291–312, 2009.

[3] Jason Leadbetter and Lukas Swan. Battery storage system for residential electricity peak demand shaving. *Energy and Buildings*, 55:685 – 692, 2012. Cool Roofs, Cool Pavements, Cool Cities, and Cool World.

[4] Michael Stadler, Hirohisa Aki, Ryan M. Firestone, Judy Lai, Chris Marnay, and Afzal S. Siddiqui. Distributed energy resources on-site optimization for commercial buildings with electric and thermal storage technologies. In *2008 ACEEE Summer Study on Energy Efficiency in Buildings, Scaling Up: Building Tomorrow's Solutions, August 17-22, 2008*, Pacific Grove, CA, 08/2008 2008. LBNL, LBNL.

[5] Andrew Wright and Steven Firth. The nature of domestic electricity-loads and effects of time averaging on statistics and on-site generation calculations. *Applied Energy*, 84(4):389 – 403, 2007.

[6] Sunliang Cao and Kai Sirén. Impact of simulation time-resolution on the matching of pv production and household electric demand. *Applied Energy*, 128:192–208, 05 2014.

[7] T. Beck, H. Kondziella, G. Huard, and T. Bruckner. Assessing the influence of the temporal resolution of electrical load and pv generation profiles on self-consumption and sizing of pv-battery systems. *Applied Energy*, 173:331 – 342, 2016.

[8] P. Stenzel, J. Linssen, J. Fleer, and F. Busch. Impact of temporal resolution of supply and demand profiles on the design of photovoltaic battery systems for increased self-consumption. In *2016 IEEE International Energy Conference (ENERGYCON)*, pages 1–6, April 2016.

[9] Alessandro Burgio, Daniele Menniti, Nicola Sorrentino, Anna Pinnarelli, and Zbigniew Leonowicz. Influence and impact of data averaging and temporal resolution on the assessment of energetic, economic and technical issues of hybrid photovoltaic-battery systems. *Energies*, 13(2):354, Jan 2020.